

Additional grain boundary strengthening in length-scale architected copper of ultrafine and coarse domains

Hou, X., Krauß, S. & Merle, B.

Author post-print (accepted) deposited by Coventry University's Repository

Original citation & hyperlink:

Hou, X, Krauß, S & Merle, B 2019, 'Additional grain boundary strengthening in length-scale architected copper of ultrafine and coarse domains' *Scripta Materialia*, vol. 165, pp. 55-59.

<https://dx.doi.org/10.1016/j.scriptamat.2019.02.019>

DOI 10.1016/j.scriptamat.2019.02.019

ISSN 1359-6462

Publisher: Elsevier

NOTICE: this is the author's version of a work that was accepted for publication in *Scripta Materialia*. Changes resulting from the publishing process, such as peer review, editing, corrections, structural formatting, and other quality control mechanisms may not be reflected in this document. Changes may have been made to this work since it was submitted for publication. A definitive version was subsequently published in *Scripta Materialia*, [165], (2019) DOI: 10.1016/j.scriptamat.2019.02.019

© 2017, Elsevier. Licensed under the Creative Commons Attribution-NonCommercial-NoDerivatives 4.0 International

<http://creativecommons.org/licenses/by-nc-nd/4.0/>

Copyright © and Moral Rights are retained by the author(s) and/ or other copyright owners. A copy can be downloaded for personal non-commercial research or study, without prior permission or charge. This item cannot be reproduced or quoted extensively from without first obtaining permission in writing from the copyright holder(s). The content must not be changed in any way or sold commercially in any format or medium without the formal permission of the copyright holders.

This document is the author's post-print version, incorporating any revisions agreed during the peer-review process. Some differences between the published version and this version may remain and you are advised to consult the published version if you wish to cite from it.

Additional grain boundary strengthening in length-scale architected copper of ultrafine and coarse domains

Xiaodong Hou^{a,b*}, Sebastian Krauß^c and Benoit Merle^c

^a*Research Institute for Future Transport & Cities, Coventry University, Coventry, Priory Street, Coventry, CV1 5FB, United Kingdom*

^b*Centre of Excellence for Advanced Materials, Songshan Lake, Dongguan, 523808, China*

^c*Department of Materials Science & Engineering, Institute 1, University of Erlangen-Nürnberg (FAU), Martensstr. 5, 91058 Erlangen, Germany*

*Correspondence to: xiaodong.hou@hotmail.com

Abstract

The strength of polycrystal is known to increase with decreasing grain size, known as Hall-Petch effect. However, this relationship fails to predict the strength of samples with a non-uniform distribution of grain sizes. In this study, we purposely designed and fabricated copper micropillars with a strongly bimodal microstructure: half volume consisted of a large number of ultrafine grains, while the other half was predominantly single-crystal. Micropillar compression evidenced that bimodal samples are 35% stronger than their counterparts containing only ultrafine grains. This paradoxical finding highlights the greater strengthening potential of microstructure distribution engineering, compared to the traditional grain refinement strategy.

Key words: grain boundary strengthening; crystal structure; Hall-Petch effect; mechanical property testing; bimodal grained microstructure

Materials scientists and engineers have been working for centuries to design and produce stronger, harder and tougher material components. In order to achieve this goal, they have mostly focused on developing a better understanding of the relationship between microstructure and mechanical performance. For metals and alloys, the classic Hall-Petch relationship [1, 2] has been a very successful expression relating the strength and grain size. Hall-Petch effect predict the increase in strength is reversely proportional to the square root of grain size, which has been the basis of a widely adopted strengthening method. Extensive efforts have been made to prepare ultrafine-grained and even nano-crystalline metals to achieve higher strength in comparison with their coarse-grained counterparts; unfortunately, a reduction in grain size often compromises the ductility of the material, hence limits their applications [3]. Furthermore, it was found that softening could occur when grain sizes were reduced to be smaller than 10 to 30 nm [4]. Nano-structured metallic multi-layer composites have also been studied as a possible route to better mechanical performance [5]. These material components indeed show high strength combined with excellent ductility [6]; but complicated methodologies are required to produce these multi-layer materials (typical individual layer thickness of around ten nanometres) hence not viable for wide industrial applications [7]. Lu etc. demonstrated that without introducing nano-layer, grain size gradient alone can achieve both strength and ductility [8, 9]. These gradient structures are generally introduced by applying a plastic deformation onto the surface of bulk coarse-grained metals; popular methods include friction sliding [10], wire

brushing [11], surface mechanical attrition/grinding treatment [12, 13], high energy shot-peening [14], etc. However, these technique also have limitations: the gradient zone normally has a relatively small thickness (typically several tens of micrometres), which puts a limit on the strengthening capability if the volume of the material components is large; the surface modification often involves severe plastic deformation, including both grain refinement and the introduction of a high dislocation density. As a result, it is not possible to separate the strengthening contributions from grain refinement and from work hardening. In additional, residual stress could also be in present in the gradient structure and play an important role in the apparent mechanical response [15]. Overall, the gradient structured materials offer great opportunity to achieve high strength and high toughness, but the underlying deformation mechanism are still not clear due to the different strengthening contribution mechanism involved (grain size, work-hardening and residual stress). Therefore, there is a genuine need to produce a new and novel material grain design to achieve the high strength and to better investigate the grain size strengthening, without having to introduce the gradient structure. In this study, we created a length-scale architected copper sample using electro-deposition method, which combined ultrafine and coarse grains domains. The aim is to develop new fundamental understanding for design rules and methods to produce stronger and tougher material components using only grain size strengthening, applicable for wide industrial application at large length-scale.

In order to create the required architected microstructure, the as-deposited fine-grain copper piece (measured mean grain size 2.4 μm) was annealed in a high vacuum furnace (600°C, 1 hour at 10^{-6} mBar) to allow the grain to grow before depositing more fine-grain copper. The surface of annealed coarse-grain copper (measured mean grain size 25.6 μm) was deeply chemically etched in the same electrolyte before depositing new fine-grain copper to remove any possible surface oxidation layer. The copper specimen was then mechanically polished, followed by a final electrolytic polishing using D2 electrolyte (Struers, Germany), in order to remove the mechanically damaged surface layers. The unique sandwich-like microstructure is shown in the Scanning Electron Micrograph (SEM) in Fig. 1, obtained using a Helios NanoLab 600i FIB workstation (Thermo Fischer Scientific, USA). Energy-dispersive spectrometer (EDS) results showed dominantly copper element, with detectable trace of carbon and oxygen, but no difference between the coarse grain, fine grain and interface. These individual constituents are respectively associated with a high strength coupled to a low ductility, and a high ductility coupled to a low strength. Electro-depositing the samples provides an ideal framework for studying the interface and bimodality effects on the strength. Unlike grading by severe surface plastic deformation, they do not introduce other strengthening contributions such as work-hardening. Pillar-shape microsamples were fabricated by focused ion-beam annular milling at carefully selected locations, using the technique described in [16-18]. An overview image of all micropillars is also shown in Fig. 1. In all, 12 micropillars were fabricated on the coarse-grained side (PCG: pillars coarse grain), 12 micropillars on the ultrafine-grained side (PFG: pillars fine grain), and 12 micropillars on the interface, i.e. containing half ultrafine-grained and half mostly single-crystalline constituents (PIF: pillar interface). The figure inset shows representative micropillars for each category. Note that the coarse-grained pillars (PCG) are mostly single-crystalline, due to the very large grain size (order of $\sim 25.6 \mu\text{m}$) in the corresponding electro-deposited layer. Their crystallographic orientation is, however, random. All these micropillars have a diameter of 5 μm , with length-to-

diameter ratio of ca. 2:5. The copper specimen was then transferred to a nanoindenter (KLA-Tencor G200 Nanoindenter, USA), and these micropillars were compressed using a flat diamond punch of 7 μm diameter to investigate their mechanical behaviour.

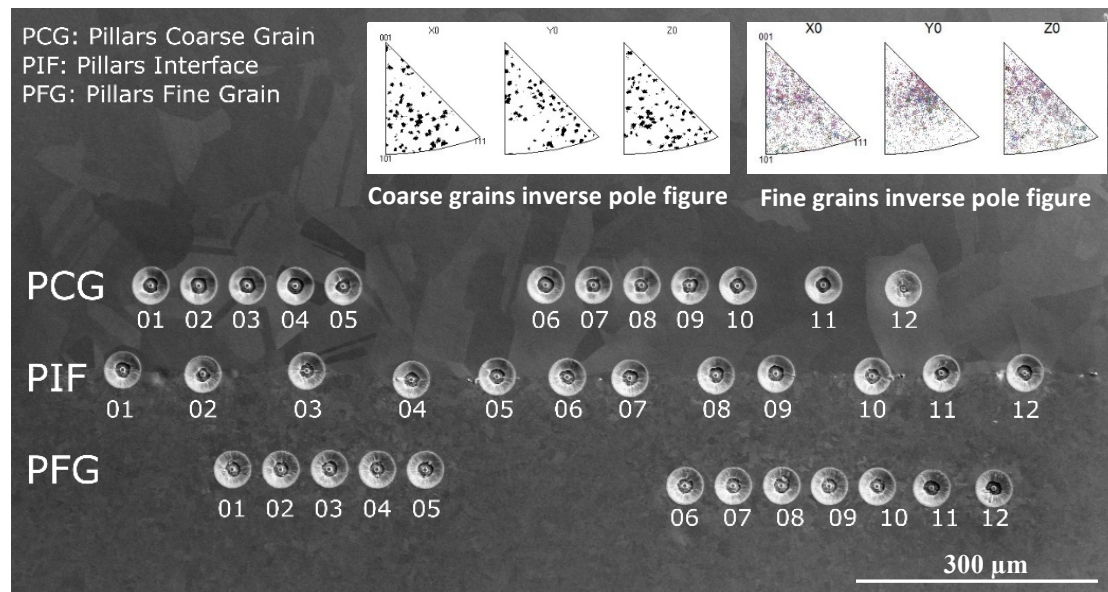


Fig. 1. Scanning electron micrograph (SEM) image overview of the length-scale architected copper sample contains coarse grain on one side and fine grain on the other side; micro-pillars made using focused ion beam (FIB) on the coarse grain (PCG: pillars coarse grain), fine grain (PFG: pillars fine grain) and interface (PIF: pillars interface). The inserted inverse pole figures show no preferred crystallographic orientation on both coarse and fine grain domains.

The experimental engineering stress-strain curves and a comparison of their yield strength $\sigma_{0.2}$ at 0.2% plastic strain are shown in Fig. 2*a-b*. As expected, these results show that the polycrystalline micropillars (PFG) are much stronger than the micropillars containing only one single grain (PCG). It is much more surprising to observe that the strength of interface micropillars (PIF) is significantly higher than the polycrystalline micropillars (PFG), which correspond to its constituent of finest grain size. It is worth pointing out that the yield strength data show large scattering, possibly due to a slight variation of the average grain size and grain orientation from sample to sample. Nevertheless, there is clearly a statistic difference between these three kinds: the PIF micropillars are definitely the strongest ($\sigma_{0.2} = 250 \pm 35$ MPa), followed by the PFG micropillars ($\sigma_{0.2} = 185 \pm 28$ MPa) and the PCG micropillars ($\sigma_{0.2} = 112 \pm 11$ MPa). SEM images of selected micropillars are shown in Fig. 3, revealing the microstructure prior to and after compression testing.

PCG coarse-grained micropillars: The PCG specimens were single crystalline – with one exception. A few of them deformed in pure single slip mode, as shown in Fig. 3 *a-b*. The corresponding specimens display a lack of strain-hardening in Fig. 2 and amount to the lowest measured strength. This evidence that after the slip system with the highest Schmid factor is first activated, dislocations travel through the whole thickness of the sample with little interactions, presumably because the density of crystallographic defects in these recrystallized PCG samples is low. Most specimens evidenced slip traces corresponding to intersecting slip systems, as shown in the representative Fig. 3*c-d*. Here, it is likely that several slip systems present similar Schmid factors, which lead to their simultaneous activation. As a result from the

dislocation-dislocation interactions, their stress-strain diagram shows some strain hardening. The shape of the stress-strain curves and the related plasticity size effect due to the relatively small pillar diameter are in reasonable agreement with the single crystal micropillars reported in the literature [19-22]. The curve with the largest hardening within the PCG group corresponds to a bicrystal. The reason is obviously that the incipiently activated slip system is blocked by the grain boundary, which explains why a multitude of different slip traces are observed on the surface of the sample. The corresponding moderate increase of the strength is consistent with expectations from literature on micropillars of similar size with a single twin or grain boundary [23-26].

PFG ultrafine-grained micropillars: Each PFG micropillar contained multiple (~100) grains. Their behaviour differed from the coarse-grained ones on at least two aspects. On the one hand, as expected from Hall-Petch relationship, they displayed a higher yield strength. On the other hand, they also evidenced a much higher strain hardening after yielding. This is an indication of an increasing dislocation storage and presumably a consequence of the activation of many slip systems in each grain in order to maintain a deformation compatible with their many neighbours. A high strengthening amount can be accumulated because – unlike with single crystalline PCG micropillars – the formation of a shear band is hindered by the many different orientations of the grains. The anisotropy of the plastic deformation sometimes causes a rotation of the grains which is most visible at the surface where the geometrical constraints are relaxed (see Fig. 3e-f). The relatively high scatter among the stress-strain diagrams shown in Fig. 2 results from local microstructural differences. Coarser samples yield at a lower strength and show less strain hardening than finer ones, because shear bands can more easily form through the whole micropillar diameter and localize deformation. The quantitative difference between the PCG and PFG could be explained using the combination of Hall-Petch effect and pillar size effect. Ehrler et al proposed a concept called “effective length” (l_{eff}), defined as the sum of reciprocal of different length scales involved in small-scale mechanical testing for interpreting mixed plasticity size effects [27], the measured flow stress σ can be expressed as $\sigma = \sigma_0 + k_{\text{HP}}/\sqrt{l_{\text{eff}}}$, where σ_0 is the yield stress and k_{HP} is the Hall-Petch constant. Applied in this case, the relevant length scales are pillar size and grain size; therefore $l_{\text{eff}} = 1/(d^{-1} + p^{-1})$, where d is the grain size and p is the pillar diameter. Taking the Hall-Petch constant as $0.14 \text{ MPa}\cdot\sqrt{\text{m}}$ [28], the grain size as $2.4 \mu\text{m}$ and the micropillar diameter as $5 \mu\text{m}$, the calculated difference between the PCG and PFG is estimated to be 47 MPa , lower than the experimental observation (approximately 73 MPa). This prediction is made by only considering the grain boundary strengthening; it was reported that the twin boundaries can also provide additional strength at this length-scale depending on the twin angle [23, 29], which could potentially account for the difference between predictions and experimental observation.

PIF bimodal micropillars: The bimodal micropillars contained a well-defined vertical interface between single-crystal and fine grained domains, see Fig. 3g-h. After compression testing, multiple slips are observed on the single-crystalline side and the interface often appears to be slightly bent. There are no current dislocation based size effect theories could be readily adapted to explain why the PIF micropillars are much stronger than their PFG and bicrystalline counterparts (see red and orange curves in Fig. 2). Specifically, the present findings cannot be accounted by the dominant Hall-Petch effect [30] nor plasticity size effect theories [31], including the strain gradient plasticity [32], dislocations starvation theory [33], and the combined length scales

theory [34]. For instance, the latter theory predicts that halving the pillar diameter would make its coarse grained domain approximately 1.4 times stronger and its fine-grained part 1.1 times stronger. These predictions fall short of accounting for the significantly larger experimental difference (see Fig. 2b). For very small grains (~ 10 nm), researchers have reported other deformation mechanisms, e.g. grain rotation [35] and dynamic process of Lomer lock formation, destruction and reformation [36]. But the grain size in this study is significantly larger than nano-grains, so these theories could not be applied directly here either.

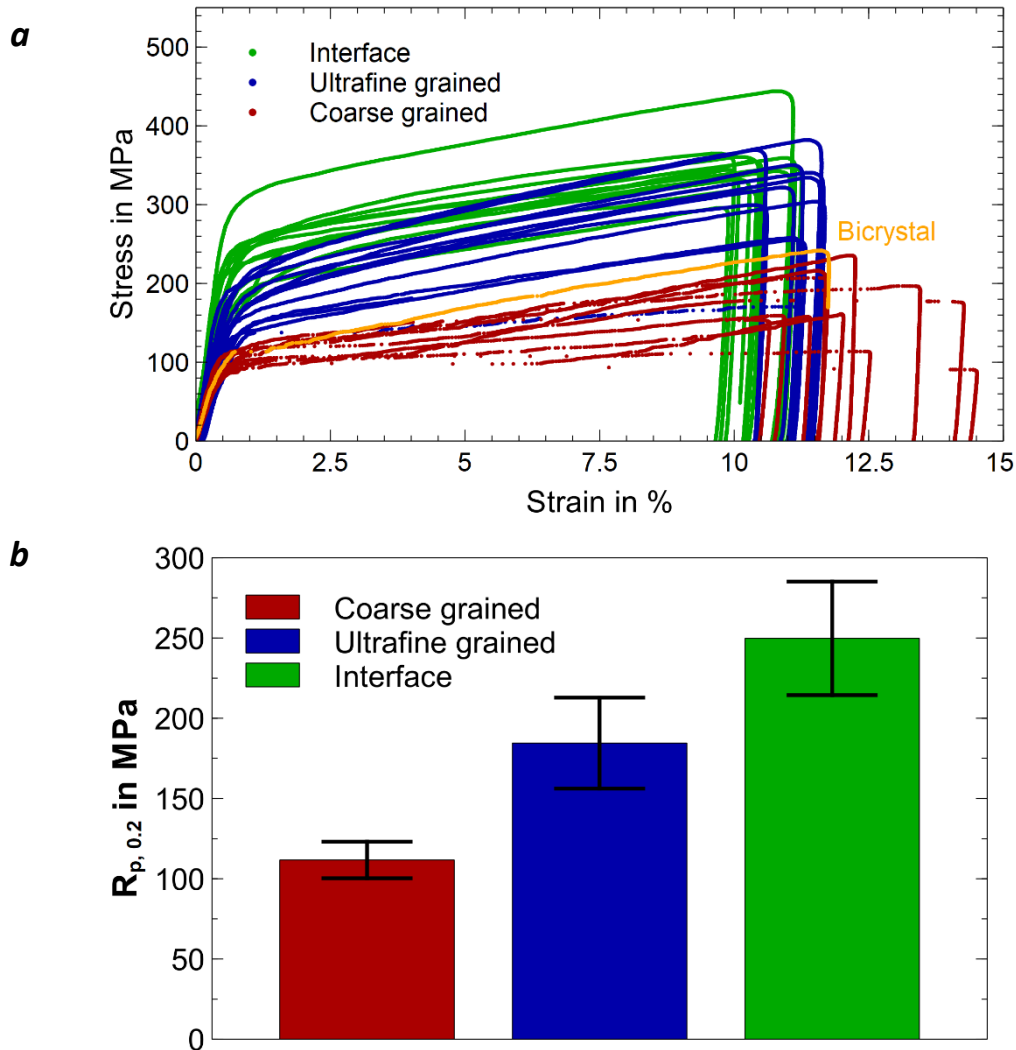


Fig. 2. Mechanical behaviour of the pure copper microsamples obtained by uniaxial micro-compression testing. (a) Stress-strain curves of 5- μ m-diameter micropillar obtained from coarse grain, fine grain and interface (in red, blue and green colour respectively). The PCG specimens were single crystalline – with one exception (in orange colour). (b) A comparison of proof engineering stress (0.2%) obtained from micropillars (σ -coarse grain < σ -fine grain < σ -interface); the error bars are calculated as standard deviation based on 12 repeated experiments for each case.

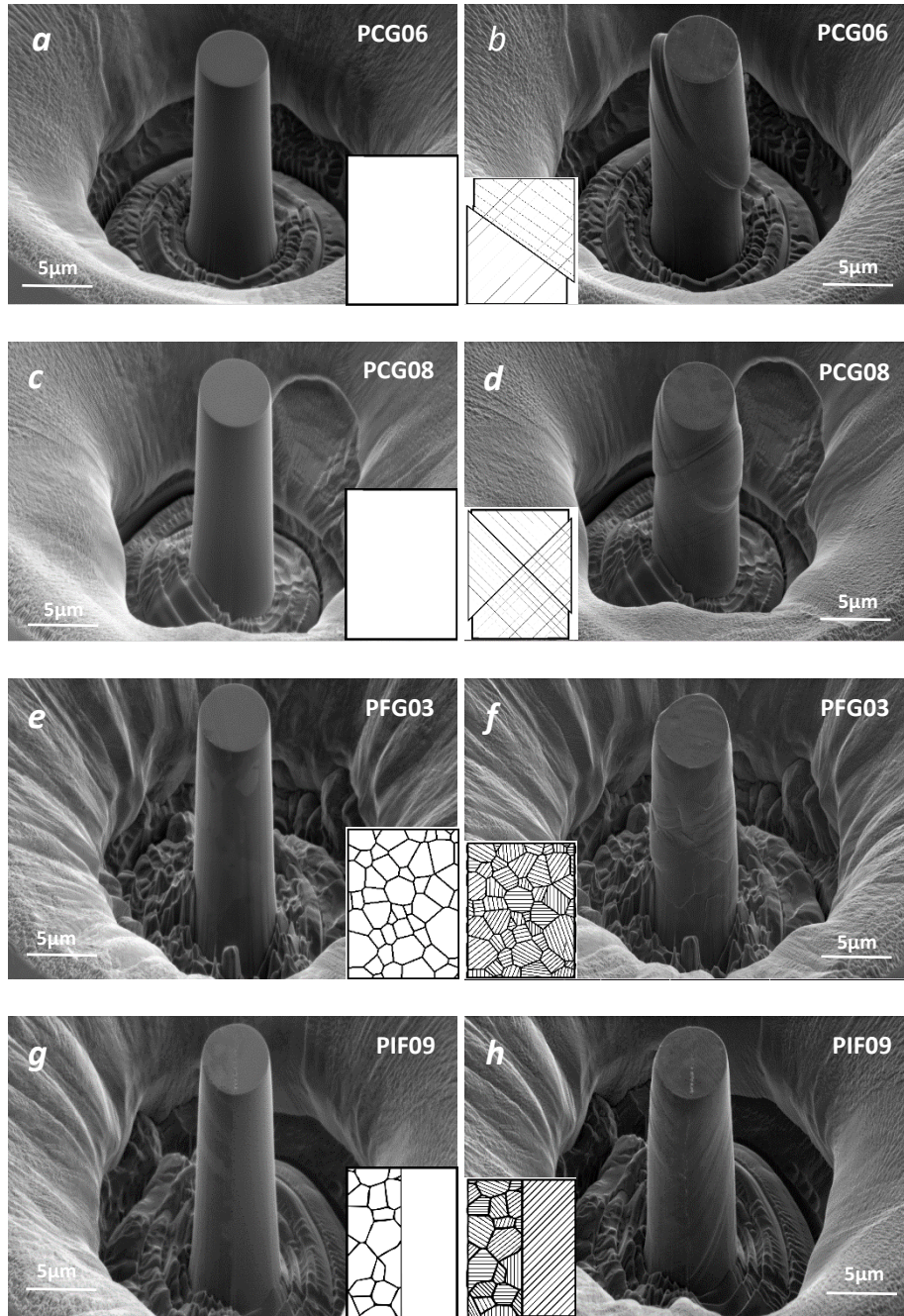


Fig. 3. SEM images of selected micropillars. (*a* to *b*) prior and post testing (PCG06) where the micropillar was cut from the coarse grain region. (*c* to *d*) Prior and post testing (PCG08) where the micropillar was cut from the coarse grain region. (*e* to *f*) Prior and post testing (PFG03) where the micropillar was cut from the ultrafine grain region. (*e* to *f*) Prior and post testing (PIF09) where the micropillar was cut from the interface between coarse grained and ultrafine grained regions.

One possible interpretation of these results is that the single-crystal part of the bimodal PIF micropillars is that reciprocal effects of the deformation in the individual domains make them both stronger than the ultrafine-grained one. It can be reasonably expected that, when subjected to compression, the single-crystalline part of the bimodal pillar would yield first, by activating a dislocation source corresponding to the slip system with most favourable Schmid factor. This shear deformation cannot, however, be immediately transmitted through the fine grained part, because many grains lying on its path are unfavourably oriented. This leads to a storage of the incoming dislocations at the interface. Following slip suppression on the first plane, the active deformation is

shifted to parallel planes, with a similar fate. This leads to the narrowly spaced parallel slip traces visible at the surface of the single crystalline part of the sample in Fig. 3*h*. Note that these events do not produce enough plastic strain to be recorded by the nano-indentation system and correspond to deformation below the macroscopic yield point in Fig. 2*a*. STEM investigations of the micropillar cross-section (see Fig. 4) evidence the storage of a large density of dislocations along the interface. It is likely that the formation of this hardened layer is pivotal in accounting for the exceptional strengthening of the bimodal micropillars. It is possible that it plays such a large role because of the anisotropic deformation of the ultrafine-grained part of the sample, which requires to locally deform this hardened single crystalline layer. Such a theory is supported by the waviness of the interface observed after testing (see Fig. 3*h* and Fig. 4*a*). In any case, the bimodal structure mostly results in a higher incipient yield strength than the ultrafine grained samples. However, following yielding, they show a weaker hardening rate. This is presumably a consequence of the lower number of grains in the sample and hence of the activation of fewer differently oriented slip systems. As with the ultrafine grained samples, the scattering of the stress-strain data is connected to the microstructure of the ultrafine grained part of the micropillar, with coarser samples corresponding to weaker samples.

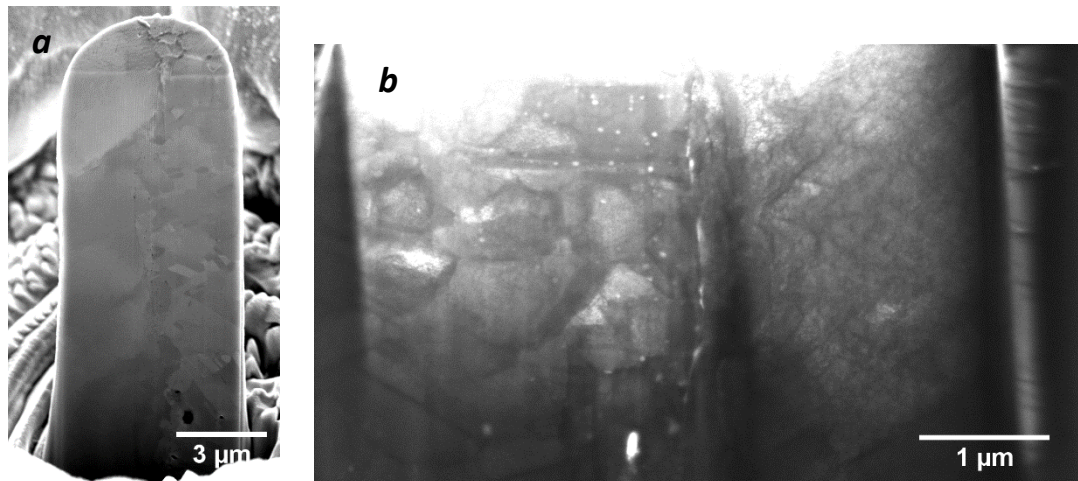


Fig. 4. Cross-section microstructure of selected deformed bimodal micropillars. (a) SEM image of the micropillar cross-section prepared by focused ion beam. (b) Scanning transmission electron micrograph (STEM) image of the lift out lamella; the dark area along the interface indicates the storage of a large density of dislocations.

In summary, the present study reveals a new strengthening effect associated with an architected micropillars made of a single-crystalline and an ultrafine grained domains are subjected to compression testing. It is shown that the interface between these domains provides additional strengthening of about 35% without compromising the ductility at small length-scales compared to an ultrafine-grained specimen.

Acknowledgements: We thank N.M. Jennett at Coventry University and A.J. Bushy at Queen Mary University of London for useful discussions. **Funding:** This work was supported by the EMPIR programme, co-financed by the Participating States and from the European Union’s Horizon 2020 research and innovation programme: Grant Number 14IND03.

References

1. E. O. Hall, Proc. Phys. Soc. B 64 (1951) 747-753.
2. N.J. Petch, J. Iron Steel Inst. 174 (1953) 25-28.
3. E. Ma, Script Mater. 49 (2003) 663-668.
4. J. Hu, Y.N. Shi, X. Sanvage, G. Sha and K. Lu, Science 355 (2017) 1292-1296.
5. N.A. Mara, D. Bhattacharyya, P. Dickerson, R.G. Hoagland, A. Misra, Appl. Phys. Lett. 92 (2008) 231901.
6. J.Y. Zhang, J. Li, X.Q. Liang, G. Liu, J. Sun, Sci. Rep. 4 (2014) 4205.
7. I. Bakonyi, L. Peter, Prog. Mater Sci. 55 (2010) 107.
8. K. Lu, Science 345 (2014) 1455.
9. X. Li, K. Lu, Nat Mater. 16 (2017) 700.
10. D.A. Hughes, N. Hansen, Phys. Rev. Lett. 87 (2001) 135503.
11. M. Sato, N. Tsuji, Y. Minamino, Y. Koizumi, Sci. Technol. Adv. Mater. 5 (2004) 145.
12. K. Lu, J. Lu, Mater. Sci. Eng. A 38 (2004) 375.
13. W.L. Li, N.R. Tao, K. Lu, Scr. Mater. 58 (2008) 546.
14. X. Zhang, N. Hansen, Y. Gao, X. Huang, Acta Mater. 60 (2012) 5933.
15. X.D. Hou, N.M. Jennett, J. Phys. D: Appl. Phys. 50 (2017) 455304.
16. M.D. Uchic, D.M. Dimiduk, J.N. Florando, W.D. Nix, Science 305 (2004) 986.
17. D.M. Dimiduk, M.D. Uchic, T.A. Parthasarathy, Acta Mater. 53 (2005) 4065.
18. B. Merle, H.W. Höppel, Exp. Mech. 58 (2018) 465.
19. N.V. Malyar, J.S. Micha, G. Dehm, C. Kirchlechner, Acta Mater. 129 (2017) 312
20. C.A. Volkert, E.T. Lilleodden, Philos. Mag. 86 (2006) 5567.
21. J.R. Greer, W.C. Oliver, W.D. Nix, Acta Mater. 53 (2005) 1821.
22. J.Y. Kim, J.R. Greer, Acta Mater. 57 (2009) 5245.
23. J.P. Liebig, S. Krauß, M. Göken, B. Merle, Acta Mater. 154 (2018) 261.
24. K.S. Ng, A.H.W. Ngan, Philos. Mag. 89 (2009) 3013.
25. T. Hirouchi, Y. Shibutani, Mater. Trans. 55 (2014) 52.
26. P. J. Imrich, C. Kirchlechner, C. Motz, G. Dehm, Acta Mater. 73 (2014) 240.
27. B. Ehrler, X.D. Hou, T.T. Zhu, C.J. Walker, A.J. Bushby, D.J. Dunstan, Philos. Mag. 88 (2008) 3043.
28. R. Armstrong, Effects of Micro-Cracking and Intrinsic Obstacle Strength on the Hall-Petch Relation for Ultrafine Grain size Polycrystals in Strength of Metals and Alloys, P. Haasen, V. Gerold, G. Kostorz G (Eds.) Proceedings of the fifth international conference on the strength of metals and alloys, Oxford: Pergamon Press, 1979, pp. 795.
29. N.V. Malyar, J.S. Micha, G. Dehm, C. Kirchlechner, Acta Mater. 129 (2017) 312.
30. D.J. Dunstan, A.J. Bushby, Int. J. Plast. 53 (2014) 56.
31. J.R. Greer, J.Th.M.De Hosson, Prog. Mater. Sci. 56 (2011) 654.
32. N.A. Fleck, G.M. Muller, M.F. Ashby, J.W. Hutchinson, Acta Mater. 42 (1994) 475.
33. J.R. Greer, W.D. Nix, Phys. Rev. B 73 (2006) 245410.
34. X. Hou, N.M. Jennett, Acta Mater. 60 (2012) 4128.
35. L. Wang, J. Teng, P. Liu, . Hirata, E. Ma, Z. Zhang, M. Chen, X. Han, Nat. Commun. 5 (2014) 4402.
36. L. Wnag, X. Han, P. Liu, Y. Yue, Z. Zhang and E. Ma, Phys. Rev. Lett. 105 (2010) 135501.